


Contents

Table of Contents	i
List of Figures	i
List of Tables	iii
0.1 VCSELs	1
0.1.1 Vertical-Cavity Surface Emitting Laser Structure	1
0.1.2 SiV center in a Vertical-Cavity Surface Emitting Laser	1
0.2 Antennas	8
0.2.1 Nanodiamond With Multiple SiV centers Coupled to Antenna	8
0.2.2 Nanodiamond With Single SiV center Coupled to Antenna	8
Index	8

List of Figures

1	(a) Sketch of the VCSEL showing the different layers.	
	ask how to cite	
2	(b) Image of the VCSEL. The circle with the black dots is the hole in the p-contact (diameter D_S , the smaller darker area in the middle is the laser output area (diameter D_A)	1
2	(a) Emission spectrum of the used VCSEL at two different currents. (b) Optical output power and voltage of the same VCSEL in dependence of input current. []	2
3	(a) SEM image of an array of VCSELs. The three wires are the anodes, which are connected to the top layer (p-contact) of the VCSEL. Therefore, three of the VCSEL structures can be operated. (b) Detail SEM image of the top of the exploited VCSEL Bm4. The circular middle part is the hole in the p-contact through which the top DBR is visible. The active diameter is smaller than that and not visible in the SEM.	2
4	(a) Scan of the VCSEL Bm4 with coupled nanodiamond under excitation with the laser from the confocal setup. The big visible ring is the edge of the circular hole in the p-contact. The bright spot in the upper left corner corresponds to the transferred nanodiamond containing an SiV center. (b) Scan of the VCSEL Bm2 without nanodiamond under excitation with the laser from the confocal setup. The circular hole in the p-contact exhibits a constant countrate.	3
5	(a) Spectrum of the preselected diamond for transfer onto VCSEL Bm4 before pick-and-place. The strong line denoted A exhibits a center wavelength of 746.0 nm and a linewidth of 1.9 nm. Line B exhibits a center wavelength of 0 nm and a linewidth of 0 nm	
	put in correct numbers	
6	(b) Spectrum of the same SiV center after pick-and-place, excited with the same laser as before. While Line A is almost gone, line B still exists and is the predominant line of the spectrum. Note: different longpass filters were used for the two measurements. Measurement (a) was performed with a 720 nm longpass filter, measurement (b) with a 710 nm longpass filter.	4
6	(a) Scan of the laser light stemming from the VCSEL Bm4 and the fluorescence light from the SiV center in the filter window 730 nm to 750 nm. (b) Scan of the laser light stemming from the VCSEL Bm2 without coupled SiV center. The outcome of the two scans is almost identical.	4

7	Reflectivity of the Distributed Bragg reflector (DBR) of the VCSEL, and spectrum of the SiV center measured during VCSEL excitation. The reflectivity of the DBR and the VCSEL emission spectra are depicted with different scales. The shape of the measurement of the SiV center during VCSEL operation coincides with the shape of the DBR reflectivity. The spectrum of the SiV center is not visible. As the emission from the SiV center is small compared to the intensity of the laser sideband in the same wavelength regime, the SiV centers emission is not detectable.	5
9	<caption>	6
10	<caption>	6
11	7
12	<caption>	7
13	<caption>	7
14	<caption>	8
15	<caption>	8
16	<caption>	9
17	<caption>	9
18	<caption>	9
19	<caption>	10

List of Tables

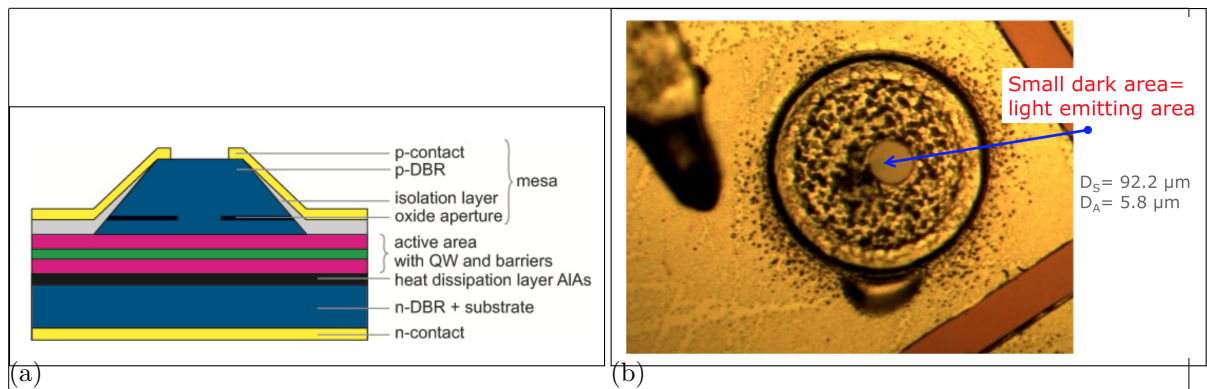


Figure 1: (a) Sketch of the VCSEL showing the different layers.

ask how to cite

(b) Image of the VCSEL. The circle with the black dots is the hole in the p-contact (diameter D_S , the smaller darker area in the middle is the laser output area (diameter D_A)

0.1 Coupling SiV centers to Vertical-Cavity Surface Emitting Lasers

For metrology, the photon flux rate has to be high enough to be measured by a low optical flux detector [?].

The red AlGaInP-based oxide-confined vertical-cavity surface emitting lasers (VCSEL) are compact and perfect candidates for excitation of SiV centers in a hybrid integrated single photon source: They exhibit wavelengths around 650 nm at continuous wave emission. SiV centers exhibit intensity maxima at an excitation at 670 nm and 690 nm []. In addition, VCSELs exhibit circular beam profile, have low divergence angle and emit linearly polarized light.

diagram
einfuegen

0.1.1 Vertical-Cavity Surface Emitting Laser Structure

The VCSEL structure (??) consists of an active region between two distributed Bragg reflectors (DBR). The bottom n-type DBR is made of 50 pairs of AlAs/Al_{0.5}Ga_{0.5}As, the p-type DBR consists of 36 Al_{0.95}Ga_{0.05}As/Al_{0.5}Ga_{0.5}As mirror pairs [?]. The active region consists of four GaInP quantum wells (QW). An oxide aperture in a field node of the standing wave serves as a spatial filter for maximum modal gain by confining the current and the optical mode. The active diameter which is defined by the oxide aperture amounts to 5.8 μm. As this region is the area where the laser emission exits the VCSEL, the nanodiamonds have to be put within this area. The used VCSEL exhibits an optical output power up to 1 mW with low threshold current of up to 3 mA at about 655 nm.

ist das
up to

0.1.2 SiV center in a Vertical-Cavity Surface Emitting Laser

As diamond material we used CVD grown nanodiamonds. They had been grown on an iridium coated silicon wafer (see ??). These nanodiamonds exhibit a nominal size of 200 nm. First, we selected a nanodiamond which exhibited one dominant line at 746.0 nm with a linewidth

nachdenken
wie for-
mulierung
richtig
ist

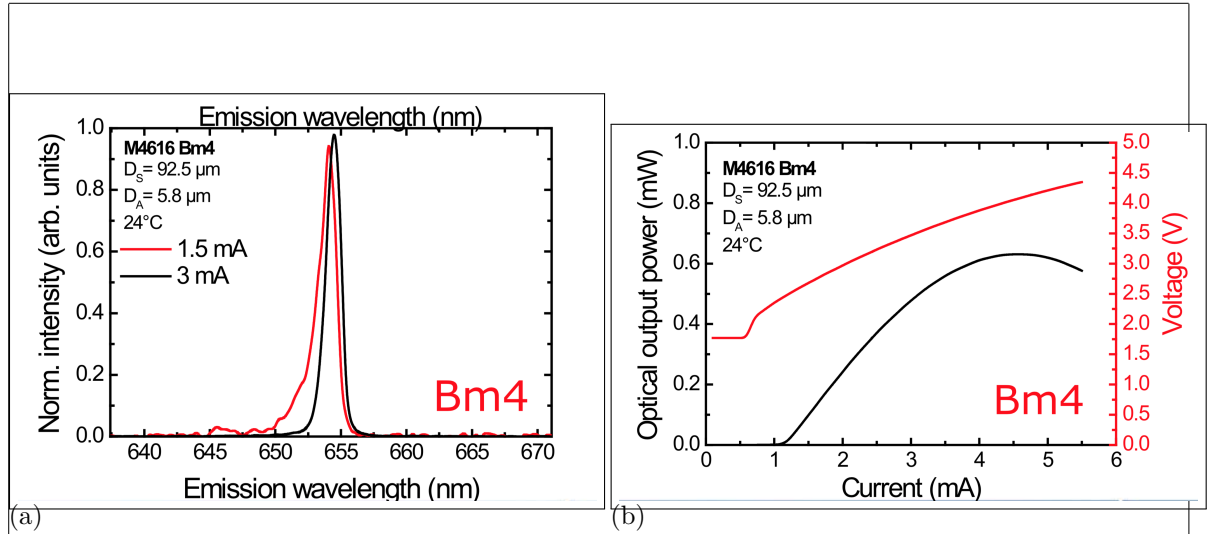


Figure 2: (a) Emission spectrum of the used VCSEL at two different currents. (b) Optical output power and voltage of the same VCSEL in dependence of input current. []

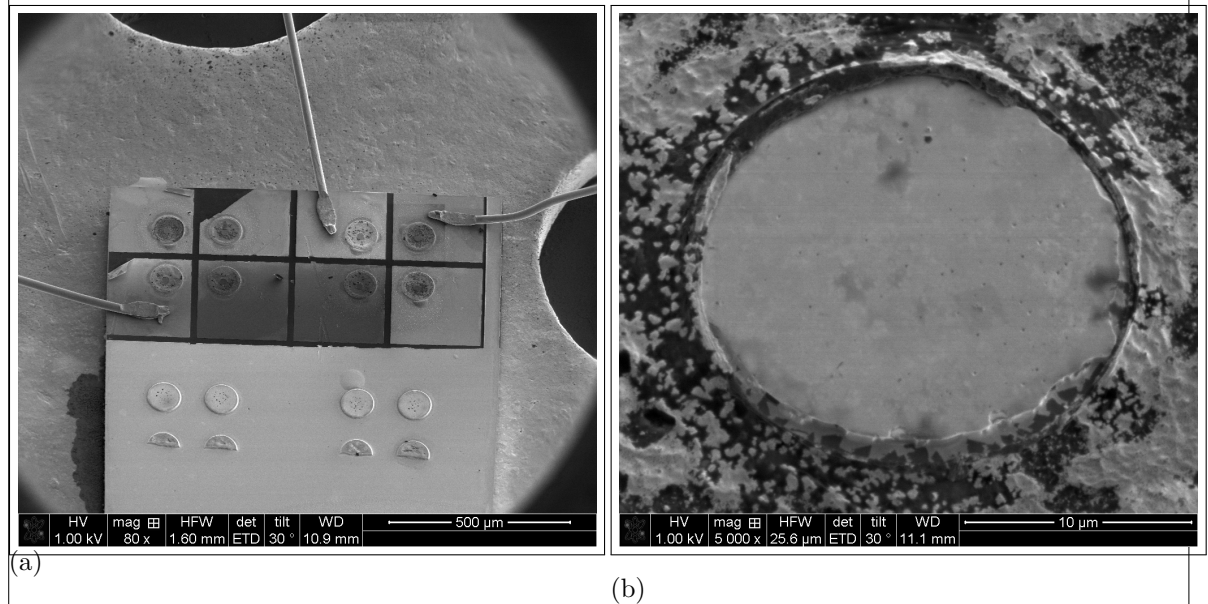


Figure 3: (a) SEM image of an array of VCSELs. The three wires are the anodes, which are connected to the top layer (p-contact) of the VCSEL. Therefore, three of the VCSEL structures can be operated. (b) Detail SEM image of the top of the exploited VCSEL Bm4. The circular middle part is the hole in the p-contact through which the top DBR is visible. The active diameter is smaller than that and not visible in the SEM.

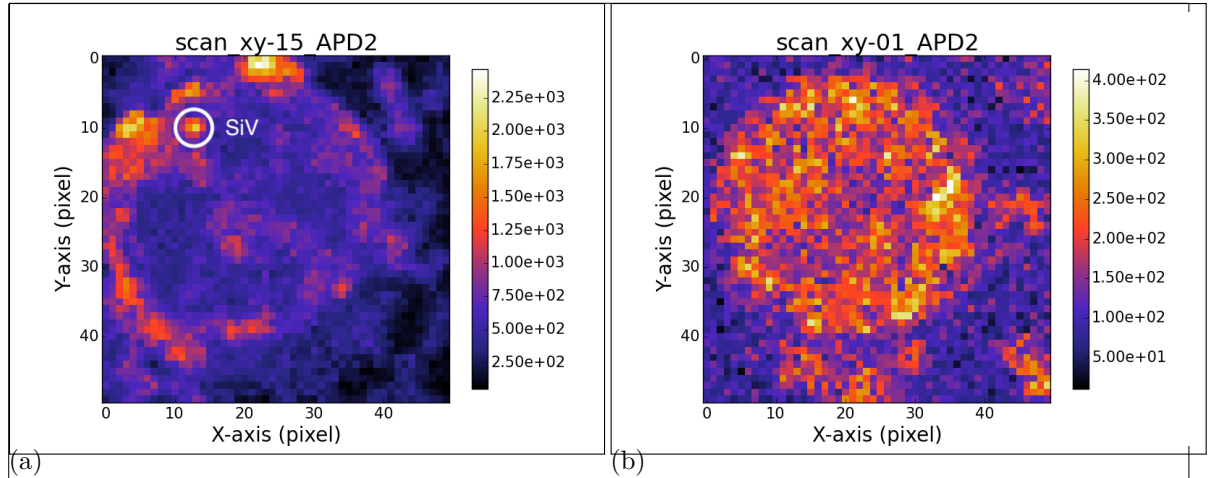


Figure 4: (a) Scan of the VCSEL Bm4 with coupled nanodiamond under excitation with the laser from the confocal setup. The big visible ring is the edge of the circular hole in the p-contact. The bright spot in the upper left corner corresponds to the transferred nanodiamond containing an SiV center. (b) Scan of the VCSEL Bm2 without nanodiamond under excitation with the laser from the confocal setup. The circular hole in the p-contact exhibits a constant countrate.

of 1.9 nm. Consecutively, its position on the substrate was determined using a white light laser scan as described in ?? . It was then transferred to the VCSEL Bm4 described in ?? . After a successful transfer of the pre-selected nanodiamond onto the active area of VCSEL Bm4, the VCSEL was put in the confocal setup. Using the laser from the confocal setup we checked if the pick-and-place process caused any modification of the spectroscopic properties of the SiV center such as a decrease of countrate or a modification of the fluorescence light spectrum. For this, the VCSEL itself was not operated itself. First, the VCSEL surface was scanned Figure 4a. . A bright dot exhibiting a countrate of a few thousand counts per second is visible where the nanodiamond containing an SiV was put. A comparative scan of a VCSEL without nanodiamond only exhibits a background countrate, as expected (Figure 4b). The spectrum of the SiV center in the transferred nanodiamond was investigated before and after the pick-and-place process (Figure 5). The original spectrum before nanodiamond transfer exhibits a sharp line at 746.0 nm (denoted line A). After the pick-and-place process, this line is still there, albeit with a low intensity. Another line at 0 nm (denoted line B) which was a minor feature in the spectrum before pick-and-place, is the predominant line after the process. This modification of the spectrum is caused by a reduction of the intensity of line A and constant intensity of line B. The reduction of the intensity of line A may be caused by damage of the color center due to electron radiation. While the energy of the electrons is low compared to the ionization energy of the color center , we observed a reduction of fluorescence light intensity after electron radiation .

was it
single?

check
number

numbers

put alex
meyers
observa-
tions in
appendix

besser
begruen-
den, was
passiert

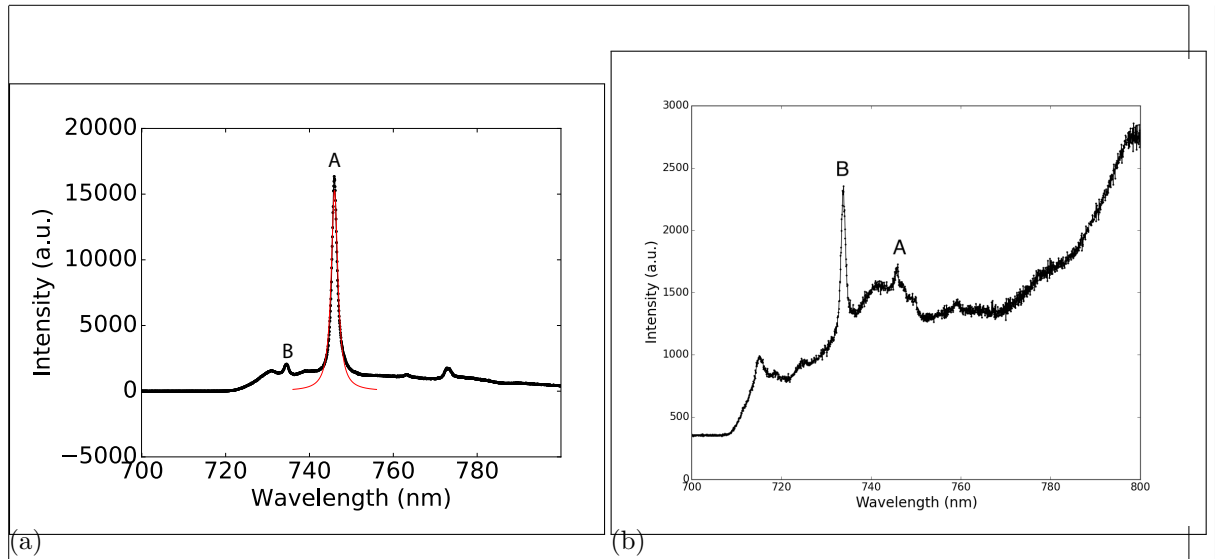


Figure 5: (a) Spectrum of the preselected diamond for transfer onto VCSEL Bm4 before pick-and-place. The strong line denoted A exhibits a center wavelength of 746.0 nm and a linewidth of 1.9 nm. Line B exhibits a center wavelength of 0 nm and a linewidth of 0 nm
put in correct numbers

(b) Spectrum of the same SiV center after pick-and-place, excited with the same laser as before. While Line A is almost gone, line B still exists and is the predominant line of the spectrum. Note: different longpass filters were used for the two measurements. Measurement (a) was performed with a 720 nm longpass filter, measurement (b) with a 710 nm longpass filter.

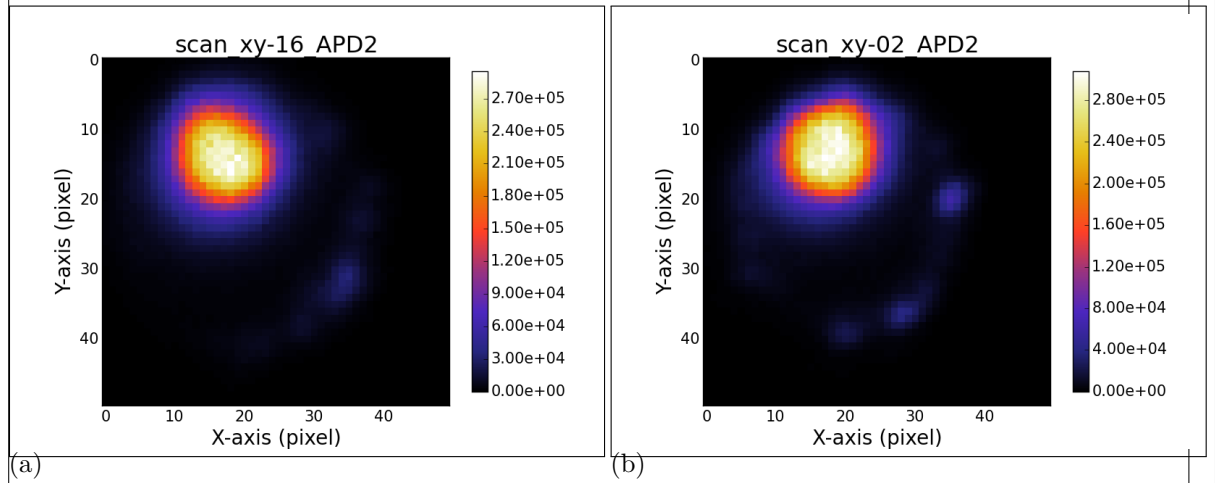


Figure 6: (a) Scan of the laser light stemming from the VCSEL Bm4 and the fluorescence light from the SiV center in the filter window 730 nm to 750 nm. (b) Scan of the laser light stemming from the VCSEL Bm2 without coupled SiV center. The outcome of the two scans is almost identical.

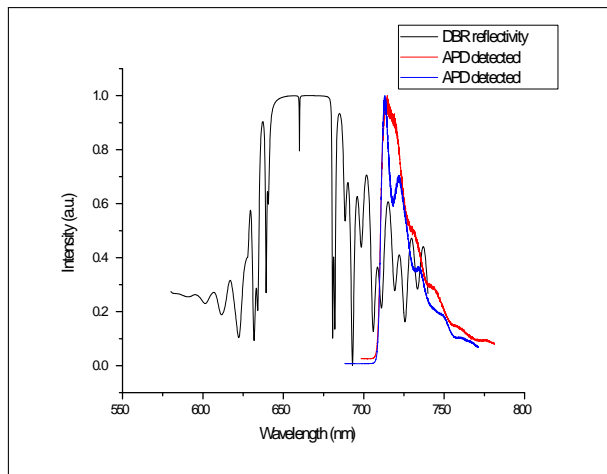
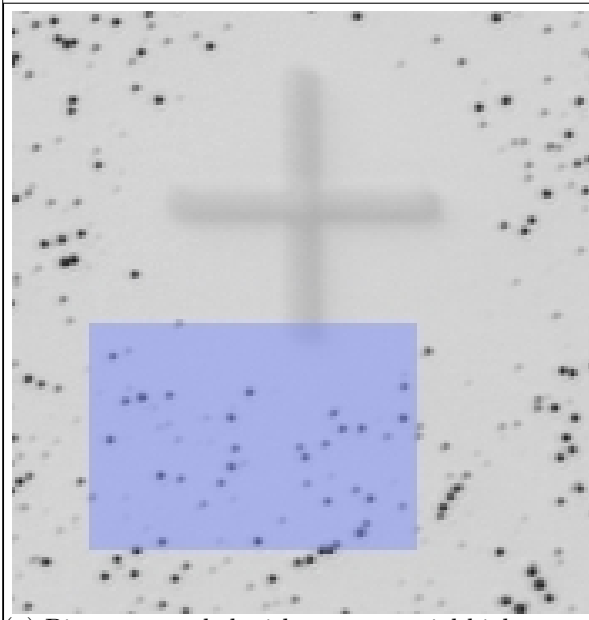
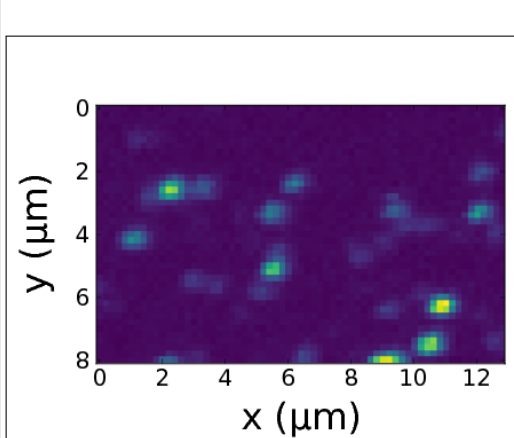


Figure 7: Reflectivity of the Distributed Bragg reflector (DBR) of the VCSEL, and spectrum of the SiV center measured during VCSEL excitation. The reflectivity of the DBR and the VCSEL emission spectra are depicted with different scales. The shape of the measurement of the SiV center during VCSEL operation coincides with the shape of the DBR reflectivity. The spectrum of the SiV center is not visible. As the emission from the SiV center is small compared to the intensity of the laser sideband in the same wavelength regime, the SiV centers emission is not detectable.



(a) Picture recorded with a commercial high resolution laser scanning microscope. The area shaded in blue represents the photoluminescence scan in image b)



(b) Photoluminescence scan of a $8 \mu\text{m} \times 13 \mu\text{m}$

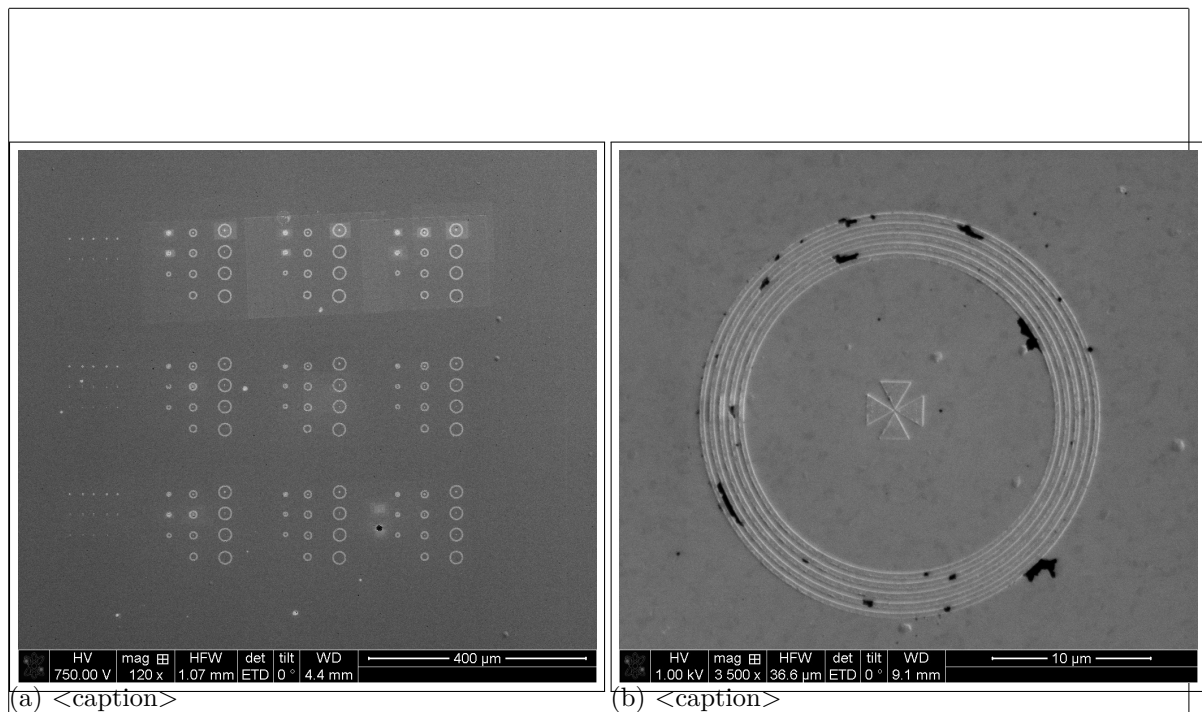


Figure 9: <caption>

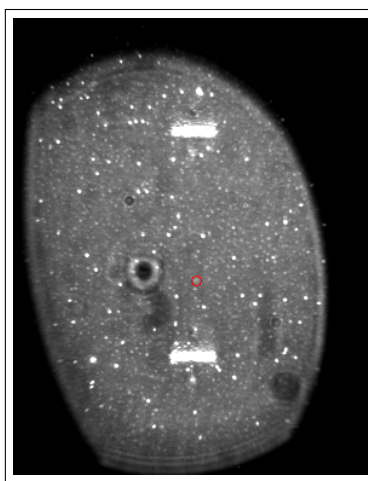


Figure 10: <caption>

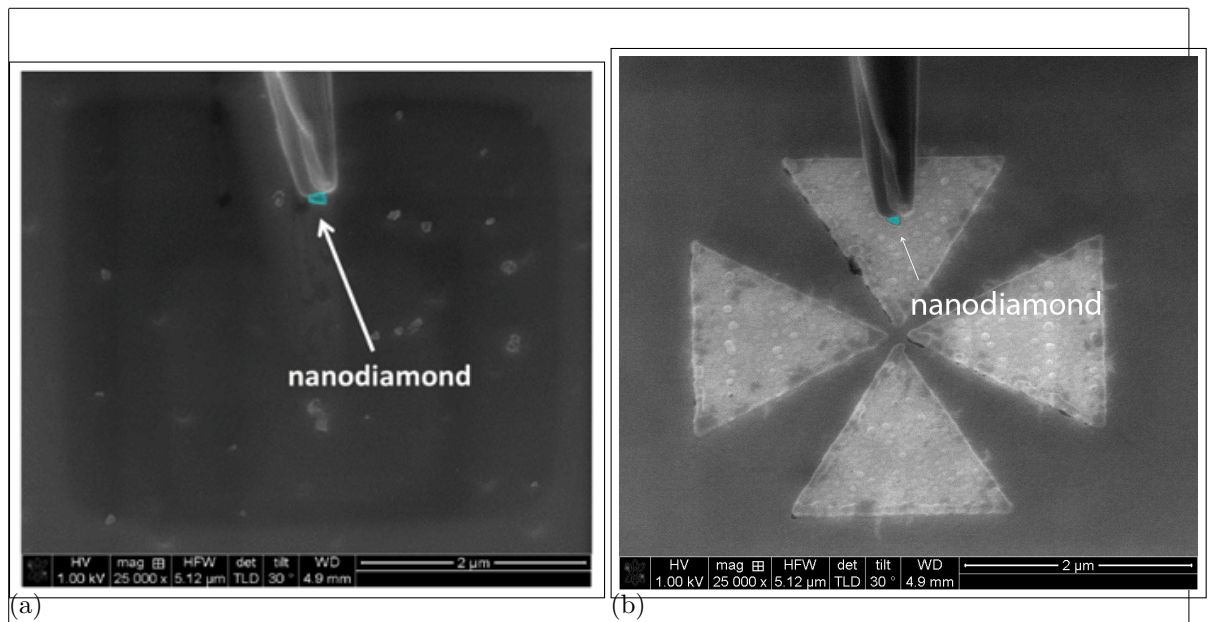


Figure 11

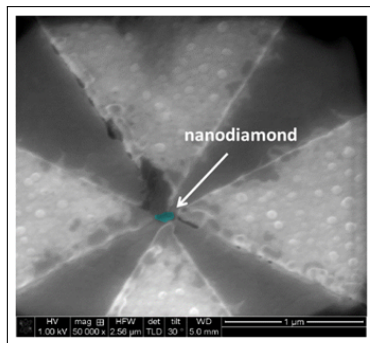


Figure 12: <caption>

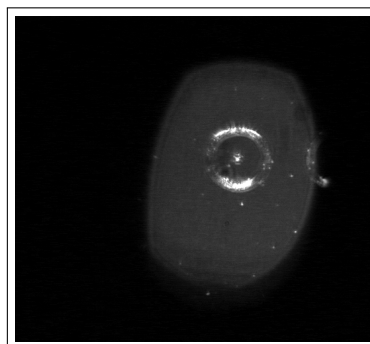


Figure 13: <caption>

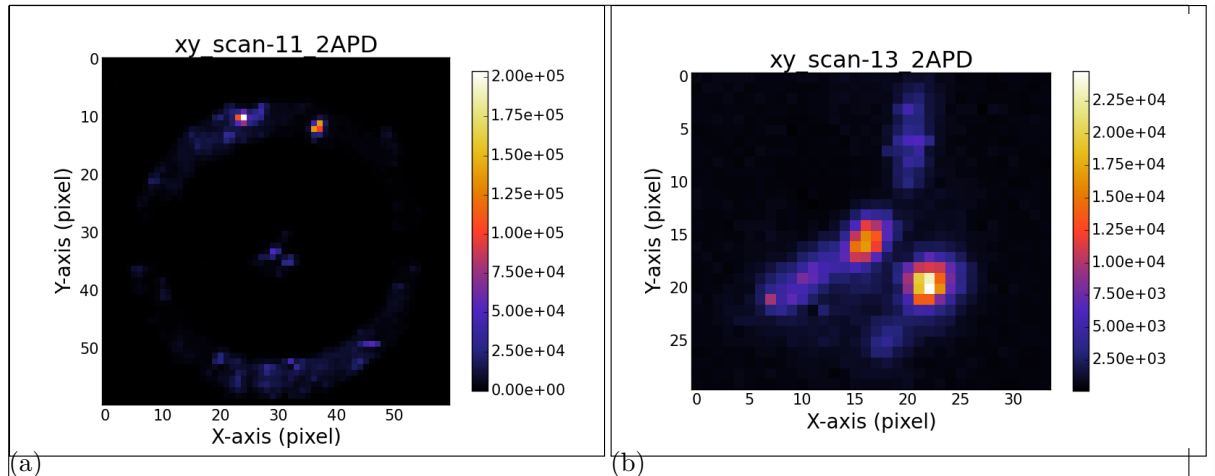


Figure 14: <caption>

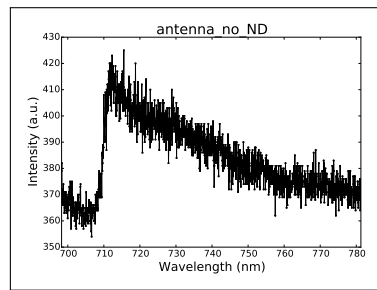


Figure 15: <caption>

0.2 Coupling Nanodiamonds to Double Bowtie Antenna Structures

0.2.1 Nanodiamond With Multiple SiV centers Coupled to Antenna

0.2.2 Nanodiamond With Single SiV center Coupled to Antenna

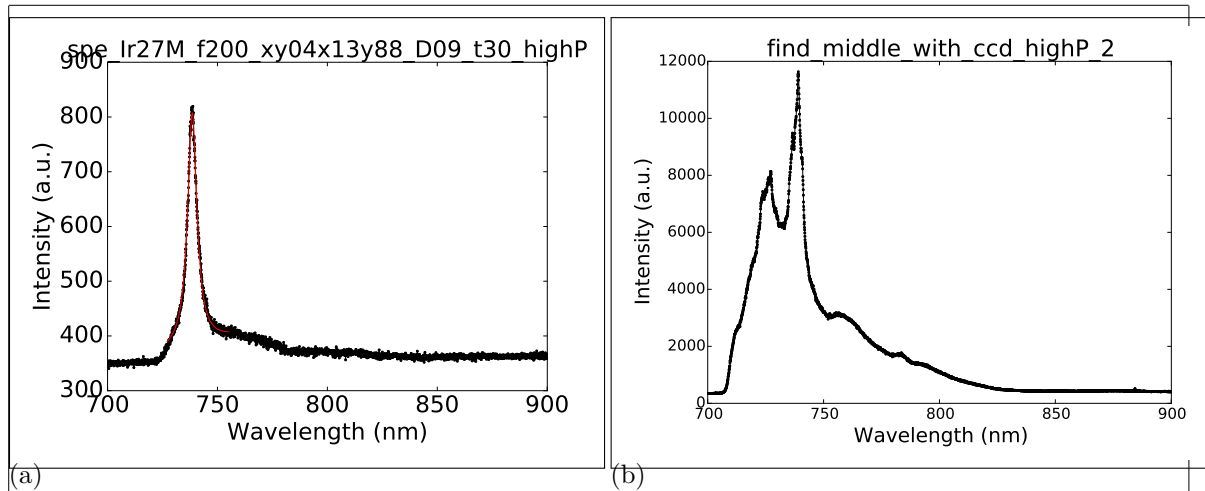


Figure 16: <caption>

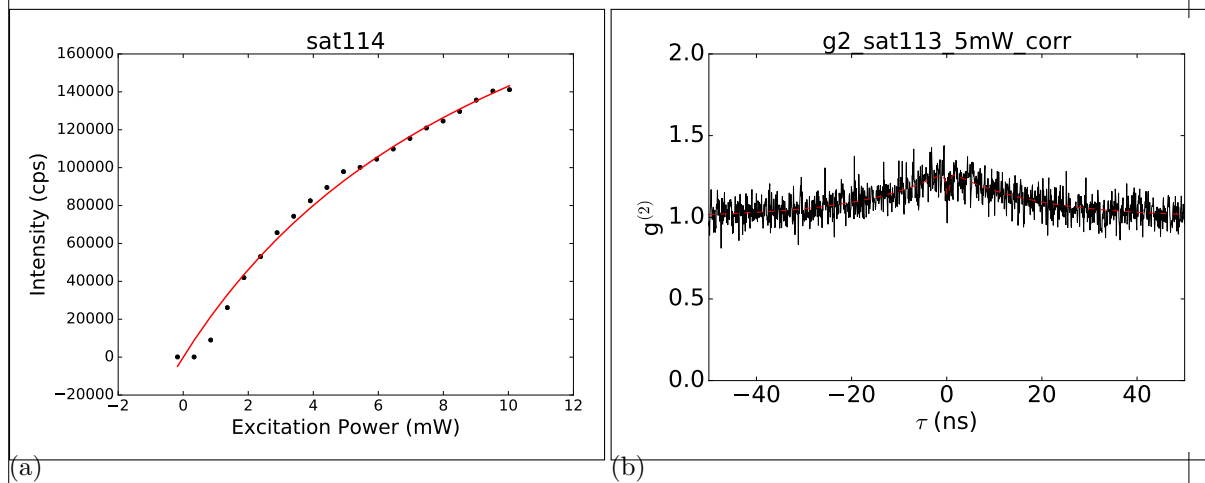


Figure 17: <caption>

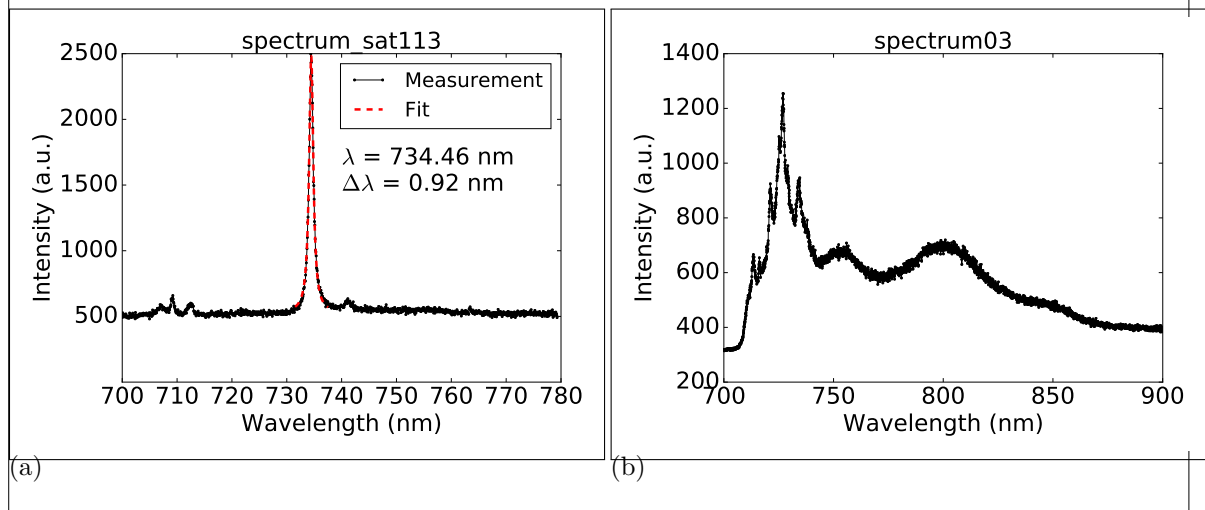


Figure 18: <caption>

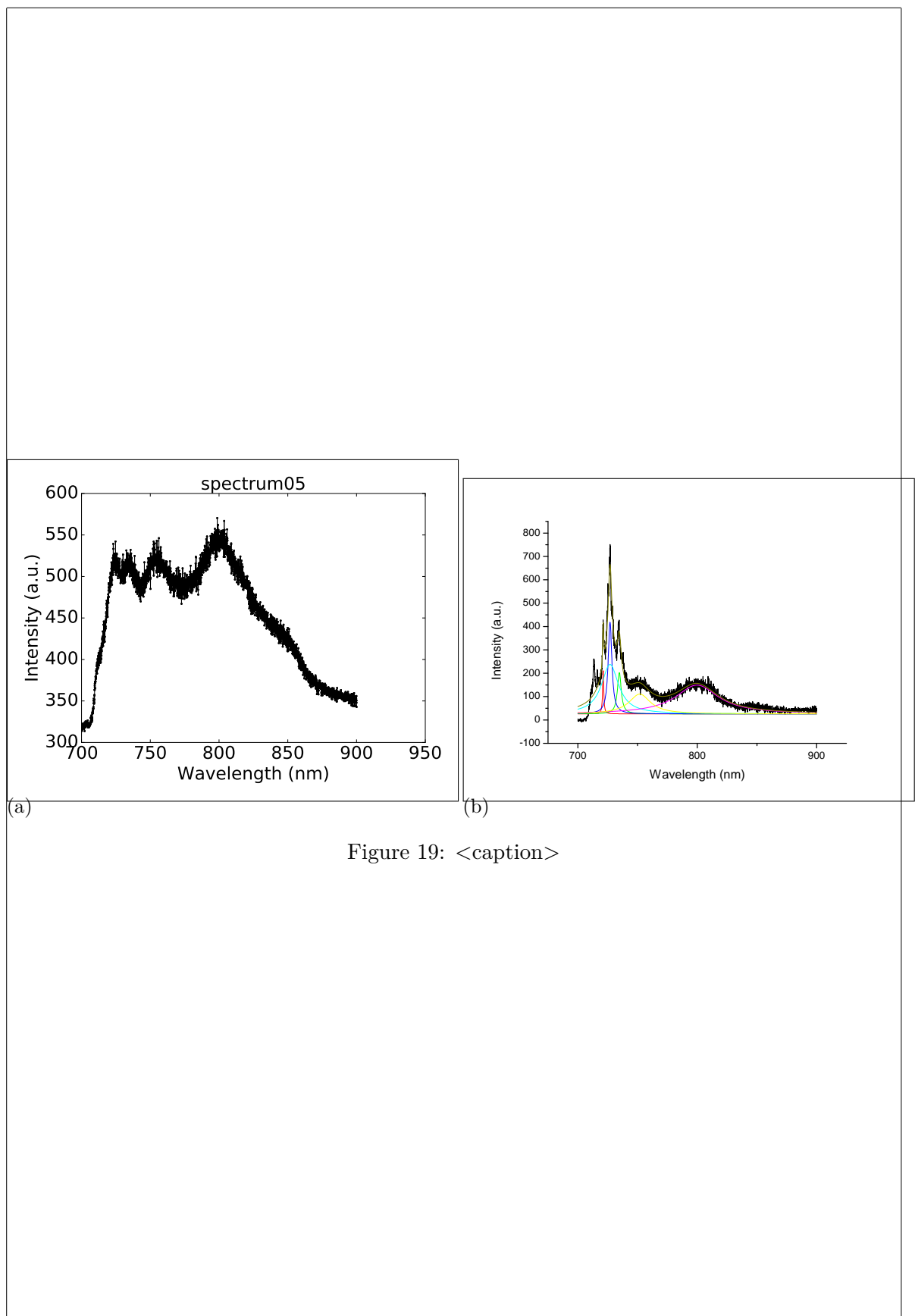


Figure 19: <caption>